

MEASUREMENTS OF AIR PERMEABILITY AND ELASTIC MODULUS OF SNOW AND FIRN DRILLED AT MIZUHO STATION, EAST ANTARCTICA*

Norikazu MAENO, Hideki NARITA and Kuniaki ARAOKA

The Institute of Low Temperature Science, Hokkaido University, Sapporo 060

Abstract: Air permeability and elastic modulus were measured for firn samples prepared from a 20-m pit and cores drilled to the depth of 147.5 m at Mizuho Station in East Antarctica. Air permeability decreased and elastic modulus increased with increasing depth or density. Two distinct changes were found at densities of 550 and 730 kg·m⁻³, *i.e.* at porosities of 0.40 and 0.20, in the plots of air permeability and elastic modulus against density or porosity. The former change is explained by the alteration of the densification mechanism from mechanical packing to plastic deformation of ice particles, and the latter by the attainment of an optimum configuration of ice bonding for air permeation and mechanical strength.

Observed results are compared with the theoretical air permeability of an ideal snow, to which all polar snows are considered to approach in a long ageing period under high hydrostatic pressure and high homologous temperature. It is suggested that the optimum state, which is reached at the density of 730 kg·m⁻³ or the porosity of 0.20, is that of snow in which air channels are mainly located at intersections of grain boundaries and some 30 percent of them are unblocked.

1. Introduction

Varieties of complex behaviors of snow originate mainly from the fact that snow is a mixture of two components, namely ice and air. Air permeability and elastic modulus can be regarded as two of the most important properties that characterize the nature of snow, because the constituent ice particles afford the mechanical strength to snow and air voids enable the permeation of various fluids through it, and hence the complicated shapes and configurations of the two components are directly reflected in the values of elastic modulus and air permeability. Consequently, careful measurements of elastic modulus and air permeability performed on the same snow samples are significant and valuable for properly understanding the behaviors of snow.

Air permeability and elastic modulus are also very important in utilizing snow as an engineering material in polar regions, so that a number of investigations for

* Contribution No. 1930 from the Institute of Low Temperature Science, Hokkaido University.

determining these parameters have been carried out so far. However, studies of natural snow in the range of high bulk densities, namely above $400 \text{ kg}\cdot\text{m}^{-3}$, are extremely few; BADER *et al.* (1955) measured the air permeability of deep-pit snow at Site 2 in Greenland to a density of $760 \text{ kg}\cdot\text{m}^{-3}$, and NAKAYA and KUROIWA (1967) to a density of $640 \text{ kg}\cdot\text{m}^{-3}$ at the same site; BENDER (1957) measured the air permeability of snow artificially compacted to a density of $490 \text{ kg}\cdot\text{m}^{-3}$.

Measurements of elastic moduli in conditions involving no macroscopic plastic deformation were made by NAKAYA (1959), and by NAKAYA and KUROIWA (1967) for the snow at Site 2 to a density of $720 \text{ kg}\cdot\text{m}^{-3}$.

For the above two reasons the present study was initiated for the purpose of gaining insight into the mechanism of the ageing process taking place in the cold polar ice sheets. The present paper reports the results of preliminary measurements of air permeability and elastic modulus carried out on snow samples collected by the 13th Japanese Antarctic Research Expedition (JARE-13) in 1972 at Mizuho Station ($70^{\circ}41.9'S$, $44^{\circ}19.9'E$; 2230 m), East Antarctica.

2. Measurements

2.1. Air permeability

The air permeability of snow samples was determined by measuring the rate of air flow and pressure difference across the sample with a permeater schematically shown in Fig. 1. The permeater is in principle similar to that used by BENDER (1957). It consists of three concentric cylinders. The outer (A) and inner (C) cylinders were fixed, and the middle cylinder (B) could be moved up and down by appropriate weights (D_1 and D_2) at a constant speed controlled with a synchronous motor (E). As the space between the cylinders (A and C) was filled with kerosene (F), the movement of the middle cylinder caused air flow through a snow sample (G).

Samples for the measurements were prepared from snow blocks collected from the walls of a 20-m pit (3 to 20 m in depth) and drilled cores of JARE-13 (20 to 60 m). By using a lathe a snow block or core was cut into a cylindrical shape; its diameter

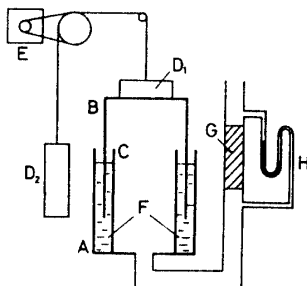


Fig. 1. Apparatus for measuring the air permeability of snow. A: outer cylinder, B: movable cylinder, C: inner cylinder, D_1 and D_2 : balance weights, E: synchronous motor, F: kerosene, G: specimen, H: manometer.

was about 5 cm and its length ranged from 2 cm to 7 cm depending upon the bulk density. The cylindrical snow sample was then wrapped tightly with a thin soft tube of rubber and connected to the permeater as shown in the figure. To obtain reproducible results special care must be taken not to leave snow fragments on the cut surfaces, and the leakage of air through the space between the sample and the rubber tube must be avoided completely by coating the sample with a thin film of ice-saturated silicone grease. Because of the limited sizes of samples provided, the direction of the air flow was not the same in all the samples, namely it was horizontal in snow samples of depths shallower than 20 m, and vertical for deeper cores.

A constant rate of air flow could be maintained in the range of $(4.6-13.7) \times 10^{-5} \text{ m}^3 \cdot \text{s}^{-1}$, which corresponds to the superficial filter velocity of $(2.1-10.8) \times 10^{-2} \text{ m} \cdot \text{s}^{-1}$, but measurements of air permeability were conducted only at velocities lower than $5 \times 10^{-2} \text{ m} \cdot \text{s}^{-1}$: at higher velocities the flow did not seem to be laminar since the plot of observed velocity against pressure difference deviated from a linear relationship. The pressure difference across the sample was measured with an inclined manometer filled with octanone or kerosene, H, when a flow in the sample attained its steady state after the initial violent oscillation of the head of the liquid filling the manometer. All the measurements were carried out in a cold room maintained at -9.0°C .

When a moderate pressure gradient, I' , is applied to an air-filled porous material and its flow is laminar, the volumetric flux, J , *i.e.*, the superficial filter velocity, u , is expressed by Darcy's law:

$$J = u = kI', \quad (1)$$

where k is the air permeability, its dimensions being $(\text{m} \cdot \text{s}^{-1})/(\text{Pa} \cdot \text{m}^{-1})$ or $(\text{m} \cdot \text{s}^{-1})/(\text{N} \cdot \text{m}^{-2})$ in SI units, which corresponds to more conventionally used units as follows: $1 (\text{m} \cdot \text{s}^{-1})/(\text{Pa} \cdot \text{m}^{-1}) = 10^3 (\text{cm} \cdot \text{s}^{-1})/(\text{dyn} \cdot \text{cm}^{-2}) = 9.807 \times 10^5 (\text{cm} \cdot \text{s}^{-1})/(\text{cmAq/cm}) (=9.807 \times 10^5 \text{ cm} \cdot \text{s}^{-1})$, but the last unit of the above four is not recommended for use because the physical meaning of permeability is not described explicitly in it. The linear relationship was found to hold fairly well unless u exceeded about $5 \times 10^{-2} \text{ m} \cdot \text{s}^{-1}$.

2.2. Elastic modulus

Elastic moduli of snow samples were measured by one of the authors (H.N.) in the glaciological laboratory at Mizuho Station, the temperature of which was maintained around -30°C in most cases. The measurements were conducted by the transversal vibration method, which has often been adopted in measurements of elastic modulus and internal friction of solid materials. The apparatus was similar to that of KUROIWA (1964), and is shown schematically in Fig. 2. A rectangular bar was cut out from a fresh snow-wall of a 20-m pit so that its long axis lay horizontally, and then thin iron plates, B_1 and B_2 , were adhered by freezing to each end

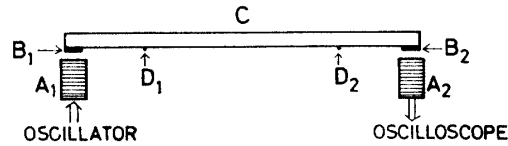


Fig. 2. Apparatus for measuring the elastic modulus of snow. A_1 and A_2 : electro-magnetic coils, B_1 and B_2 : thin iron plates, C : snow sample, D_1 and D_2 : fine strings.

of the bar. The length of the bar was 20.0 cm and its width ranged from 2.2 cm to 3.5 cm and its thickness from 0.8 cm to 2.2 cm, the dimensions corresponding to resonant frequencies of 290 to 840 Hz depending upon the densities. The bar was supported with two fine strings stretched horizontally, D_1 and D_2 , at its nodal points of vibration. It was forced to oscillate by supplying alternating current to the exciting magnet, A_1 , and the resonant frequency was determined by monitoring the electric current induced in the pick-up coil A_2 .

The lateral vibration of a rectangular bar with energy dissipation due to internal friction was solved by YOSIDA *et al.* (1956); the amplitude of vibration, A , attenuates with a damping coefficient, λ ,

$$A = A_0 \exp(-\lambda t) \sin \omega t, \quad (2)$$

where A_0 is a constant, and the angular frequency, ω , is written as

$$\omega^2 + \lambda^2 = \frac{h^2 m^4 v^2}{12l^4}. \quad (3)$$

Here h and l are respectively the thickness and length of the bar, v is the velocity of sound in the material, and m is a constant, 4.730 for the fundamental mode and 7.853 for the first overtone, determined by the mode of vibration. In the present measurements the amplitude is small and temperature is low so that λ^2 is negligible compared with ω^2 in eq. (3), and if the rectangular snow bar is assumed to be a homogeneous material with a bulk density, ρ , its elastic modulus, E , is written as

$$E = \rho v^2 = \frac{48m^2 f^2 l^4 \rho}{h^2 m^4}, \quad (4)$$

where $f = \omega (2\pi)^{-1}$. This relation is identical with that obtained by RAYLEIGH (1929) for elastic vibration without internal viscosity. The bulk densities of snow samples were measured after the resonance frequency experiments.

3. Air Permeability of the Mizuho Cores

Air permeabilities observed for the Mizuho cores are plotted against depth in Fig. 3. It is seen that air permeability decreases with increasing depth, and that its rate decreases principally at two points, namely around 8 m and 30 m in depth, which are depicted as A and B. In the figure the density of snow, which was averaged

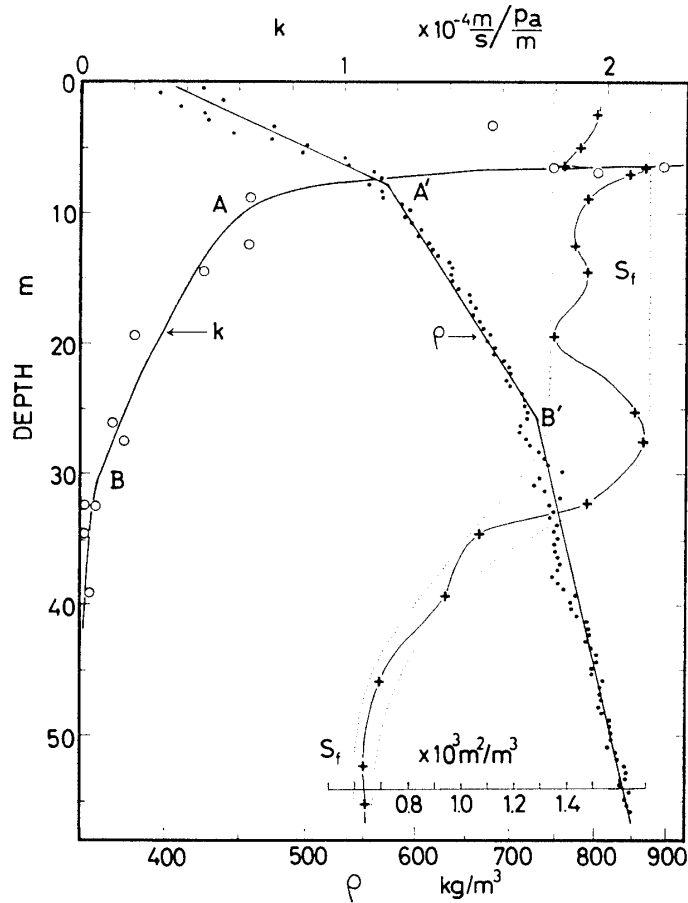


Fig. 3. Air permeability (k) plotted against the depth, together with the bulk density (ρ) and specific area of internal free surfaces (S_f).

at 0.5 m intervals (NARITA and MAENO, 1978), is also plotted. It seems that the two kinks, A and B, observed in air permeability, are related to those appearing in the density profile, A' and B'; it is reported that at a critical density around $550 \text{ kg} \cdot \text{m}^{-3}$ the densification mechanism changes from mechanical packing of air space with ice grains to plastic deformation of ice particles (BENSON, 1962; ANDERSON and BENSON, 1963). It is also reported that at another critical density around $730 \text{ kg} \cdot \text{cm}^{-3}$ the bonding and packing mode of component ice particles reaches its maximum or optimum state *i.e.*, the contact between constituent ice particles is maximum (MAENO, 1974a, 1974b, 1978).

The rapid decrease in air permeability in the top 30 m suggests the splitting and blocking of air channels within snow. This is in agreement with the almost constant value of the specific area of internal free surface (ice-air interface), S_f , shown in Fig. 3, which was measured in photomicrographs of thin sections of cores (NARITA *et al.*, 1978).

The depth of zero-permeability could not be determined by the present apparatus, because values of air permeability of snow samples recovered from depths deeper than about 40 m were too small to be measured accurately. But the linear plot of the measured values against density or porosity suggests that the air permeability becomes nearly zero as the depth approaches 55 m, *i.e.*, the density or porosity approaches $840 \text{ kg} \cdot \text{m}^{-3}$ or 0.10, respectively. Here the porosity (p) is defined as $p = 1 - (\rho/\rho_1)$ where ρ and ρ_1 are the densities of the sample and solid ice.

Fig. 4 gives the logarithmic plot of air permeability as a function of density. The distinct change at the density of $730 \text{ kg} \cdot \text{m}^{-3}$ (porosity, 0.20) should be noted. The drastic change seems to correspond to the rapid change of S_f at 30 m in Fig. 3.

Fig. 5 shows the same plot against porosity of a snow sample, together with the results obtained for natural snow drilled at Site 2 in Greenland (BADER *et al.*, 1955; NAKAYA and KUROIWA, 1967) and artificially compacted snow (BENDER, 1957). By combining the results obtained at the same place by these authors, the dependence upon porosity of air permeability of snow at Site 2 can be divided into three parts as described as a broken line with turning points A and B; the points lie at porosities of 0.40 and 0.20, which correspond to densities of 550 and $730 \text{ kg} \cdot \text{m}^{-3}$, respectively. Though the original authors did not notice these two turning points of air permeability, the present authors consider that they are quite important in understanding the physical and historical characteristics of internal structures of snow in polar ice sheets.

Particularly it must be noted that an abrupt change of air permeability was found at a porosity of 0.20, *i.e.* at the density of $730 \text{ kg} \cdot \text{m}^{-3}$, in both Antarctic and

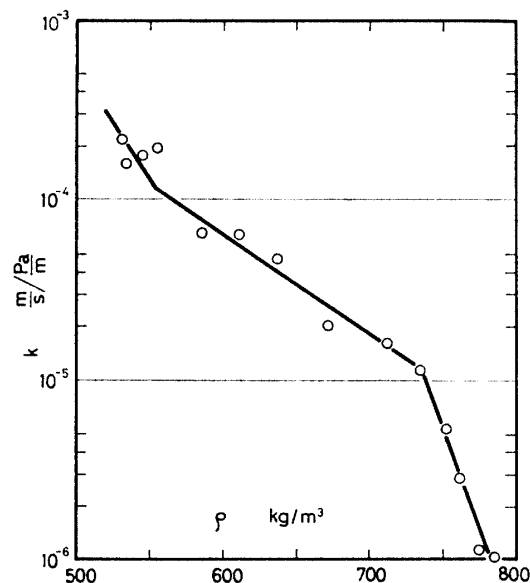


Fig. 4. Air permeability (k) versus density (ρ).

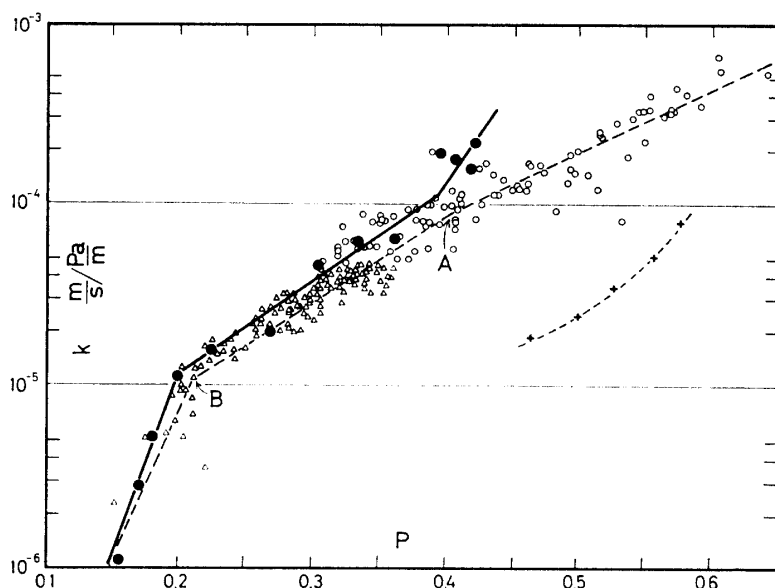


Fig. 5. Air permeability (k) plotted against porosity (p). ●: present measurements, Δ and \circ : natural snow at Site 2 in Greenland, data obtained by BADER *et al.* (1955) and NAKAYA and KUROIWA (1967), respectively, +: artificially compressed snow (BENDER, 1957).

Greenland snows. This suggests that the completion of some optimum configuration at the critical porosity is not a special phenomenon occurring only in the Mizuho region but rather a more general one which is presumably common to all the cold polar glaciers. If this is the case, other physical properties such as electrical, structural and mechanical properties might also change at this porosity; this kind of study is urgently required for other polar glaciers.

In Fig. 5 the values of air permeability obtained by BENDER (1957) are given for snow which was over a year old and artificially compacted; the values are smaller by an order of magnitude than those of natural Mizuho and Site 2 snows of the same porosity. This implies that the natural ageing or annealing process lasting over a few hundreds of years has caused the shapes and configurations of air voids within snow to transform into more favorable ones for permeation of air. This process may not be the simple spheroidization and growth of composing ice grains, as manifested clearly in the sophisticated features of grains and voids in the cores (NARITA *et al.*, 1978). This subject will be discussed in more detail in Section 5.

4. Elastic Modulus of the Mizuho Cores

Fig. 6 shows elastic moduli (E) of snow samples plotted against depth, together with the specific area of crystallographic grain boundaries (S_g) which was measured in photomicrographs of thin sections under polarized light (NARITA *et al.*, 1978). Though the observed results of E are scattered the general tendency is toward an

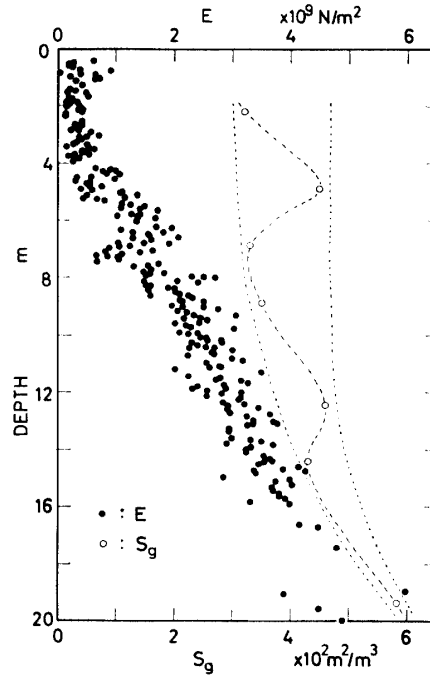


Fig. 6. Elastic modulus (E) versus depth, together with the specific area of crystallographic grain boundaries (S_g).

increase with the depth; the increase can be explained qualitatively as caused by the addition of density, and the scatter is considered to reflect the variation of internal textures such as sizes of grains, extent of bond growth between them, and so on. This explanation is in accordance with the complex fluctuation of S_g , which also increases with increasing depth.

Values of elastic modulus were plotted as a function of density in Fig. 7. The two solid straight lines, X-Y-Z, are the regression lines obtained by the least square method, which are

$$\log E = 5.75 \times 10^{-3} \rho + 6.02, \text{ for } \rho \leq 550 \text{ kg} \cdot \text{m}^{-3} \quad (5)$$

and

$$\log E = 3.40 \times 10^{-3} \rho + 7.30, \text{ for } \rho > 550 \text{ kg} \cdot \text{m}^{-3}. \quad (6)$$

Although these empirical equations should be regarded as only a crude approximation, the change of the relationship around a density of $550 \text{ kg} \cdot \text{m}^{-3}$ is significant as already noticed in the permeability measurements. In analogy to the density dependence of air permeability, the relation between elastic modulus and density, namely eq. (6), is expected to alter at the critical density of $730 \text{ kg} \cdot \text{m}^{-3}$.

The curve L-M-N in Fig. 7 gives the empirical relation obtained at -9°C by NAKAYA (1959) for deep-pit snow at Site 2 in Greenland. The empirical equations are written in SI units as

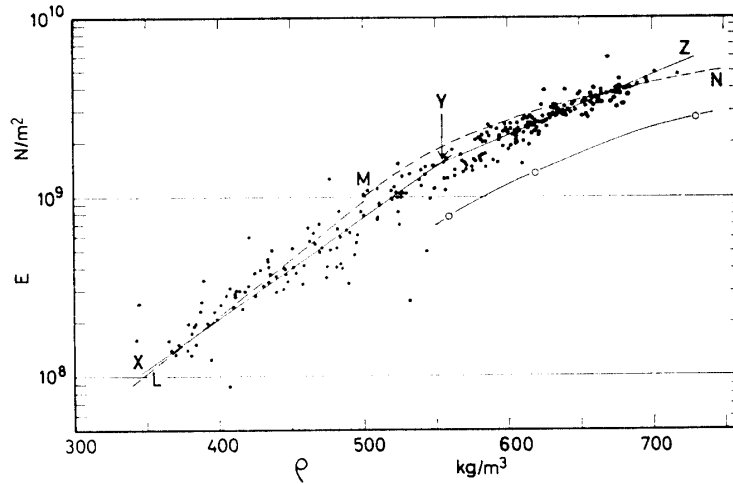


Fig. 7. Elastic modulus (E) versus density (ρ). The solid line X - Y - Z is the regression lines of eqs. (5) and (6) in the text. The dashed line L - M - N indicates the empirical results, eqs. (7) and (8), obtained by NAKAYA (1959). Open circles are the results of KUROIWA and KAWAMURA (1974) for artificially compressed snow.

$$\log E = 5.80 + 6.35 \times 10^{-3} \rho, \text{ for } 250 < \rho < 500 \text{ kg} \cdot \text{m}^{-3}, \quad (7)$$

and

$$E = (1.64\rho - 720) \times 10^7, \text{ for } 500 < \rho < 900 \text{ kg} \cdot \text{m}^{-3}. \quad (8)$$

Below a density of about $500 \text{ kg} \cdot \text{m}^{-3}$ elastic moduli of the Mizuho cores can be described roughly with a line L - M . In other words, eq. (7) can be regarded as identical with eq. (5) ascribing the scatter to variations of internal textures. But at densities between 500 and $680 \text{ kg} \cdot \text{m}^{-3}$ the deviation of the Mizuho data from the curve M - N is fairly large. The reason for the deviation is not the difference in snow and measurement temperature between NAKAYA's and the present experiments; the elastic moduli obtained by NAKAYA himself were also smaller than those predicted by eq. (8) in the density range in question (see Figs. 12 and 16 in NAKAYA, 1959). This seems to suggest that the elastic modulus in this range does not depend linearly upon the density as assumed by NAKAYA, but depends more strongly as given by eq. (6). This conclusion is in harmony with the rapid decrease in air permeability in this density range (Fig. 4).

Three open circles in Fig. 7 give the elastic moduli of artificially compressed snow measured at -30°C by KUROIWA and KAWAMURA (1974). They are much smaller than those of Antarctic snow, suggesting that bonding between ice particles has not developed very much.

5. Discussion

In the ageing process of snow in polar ice sheets, constituent ice particles and

air voids vary their shapes and configurations together with the gradual increase in the bulk density of snow. Needless to say, the ageing process is subject to the requirement that the total free energy of the system decreases toward some minimum value, but it is not certain what shapes and configurations of ice particles and air voids are the most stable in the thermodynamical sense.

As ageing proceeds, the bulk density of snow increases so that ice bonding develops and air space decreases. Accordingly, the elastic modulus increases and air permeability decreases. However, the results of the present measurements of snow at Mizuho Station suggest that, during the densification process ice particles and air voids transform to some kind of shapes and configurations which may give the maximum values of elastic modulus and air permeability at each density and porosity, and it is also found that such optimum shapes and configurations for mechanical strength and air permeation are attained at a critical density of $730 \text{ kg} \cdot \text{m}^{-3}$ or porosity of 0.20.

The attainment of such an optimum state at the critical density was first proposed by MAENO (1974a, 1974b, 1978), who studied the electrical properties of Mizuho cores. Though we have not found what kind of geometrical configuration is the final one to which the air voids and ice framework approach in a long ageing period in the polar ice sheets, a preliminary discussion will be presented below with special reference to air permeability.

We assume an ideal isotropic mixture of ice and air, in which interconnecting ice particles and air channels are randomly distributed. Let each air channel be idealized as a cylinder of radius r and the flow in it be of Hagen-Poiseuille type; then the volumetric rate of flow through a channel, q , is written as

$$q = \frac{\pi r^4}{8\eta} (\Gamma \cos \phi), \quad (9)$$

where η is the viscosity of air and ϕ is the angle between the channel and the general direction of the pressure gradient, Γ . By taking the random configuration of channels into account, the space average of $\cos \phi$ in all directions is calculated as $\overline{\cos \phi} = 1/2$, so the volumetric flux through a unit cross-sectional area of the mixture is

$$J = \frac{\alpha n \pi r^4}{16\eta} \Gamma, \quad (10)$$

where α is the fraction of channels which are unblocked, and n is the number of channels crossing the unit area.

In stereology the total length of random lines per unit volume is calculated to be equal to twice the number of points of intersection with a test plane per unit area (UNDERWOOD, 1970), so that in the present case the porosity of the ideal snow is expressed as

$$p = 2n\pi r^2. \quad (11)$$

Consequently, by comparing eqs. (10) and (11) with eq. (1), we obtain the air permeability, k , as

$$k = \frac{\alpha p r^2}{32 \eta} \quad (12)$$

Shapes of air channels in snow are generally very complicated so that their radii are very difficult to define and estimate; in the present measurements such complex air voids appearing in microphotographs of thin sections of core samples were split into several circles of equivalent areas and the frequency distribution of their radii was obtained. Some examples are shown in Fig. 8 and their arithmetic mean radii are plotted against porosity in Fig. 9. This estimate of radii of air voids is certainly a crude one, but seems to be reasonable in taking into account that circular cross sections are most favorable for flow of fluids through channels.

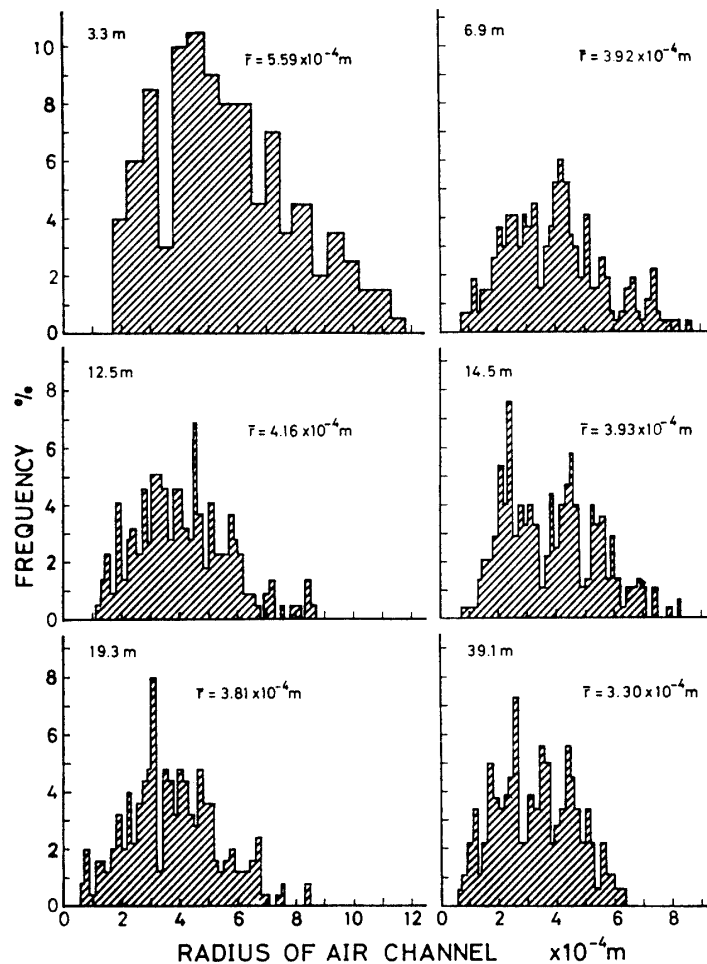


Fig. 8. Histograms of radius of air voids in the Mizuho cores. The arithmetic mean radius, \bar{r} , is also shown.

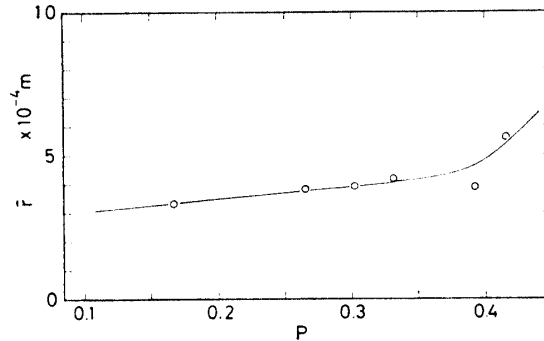


Fig. 9. Mean radius (\bar{r}) of air voids versus porosity (p) for the Mizuho cores.

In Figs. 8 and 9 it is apparent that, as the depth increases or the porosity decreases, larger air voids diminish and the mean radii decrease, roughly from 6×10^{-4} m to 3×10^{-4} m. This suggests in general the splitting and spheroidization of air voids due to the development of bonds between ice particles. The transformation of air voids to smaller ones is clearly reflected in the almost constant specific area of internal free surfaces (S_f) in Fig. 3.

The sharp change of the mean radius at the porosity of 0.4 seems to be in agreement with that observed in air permeability (A in Figs. 3 and 5), elastic modulus (Y in Fig. 7) and density (A' in Fig. 3), implying that the change of the densification mechanism at this density is also reflected in the shapes and sizes of air voids. It should be noted in Fig. 8, however, that all the histograms obtained do not give a simple one-maximum distribution but they rather seem to give two-maximum one, especially for the sample of 14.5 m in depth; in this respect more detailed analyses of air voids are in progress.

Now that the mean radius of channels in the real Antarctic snow is known, we can estimate the air permeability of an ideal mixture snow in which air channels are randomly distributed. Fig. 10 gives the theoretical air permeability of ideal snow as a function of p and αr^2 , which was calculated from eq. (12) by taking the viscosity of air to be $\eta = 1.67 \times 10^{-5}$ N·s·m $^{-2}$ at -10°C (SMITHSONIAN INSTITUTION, 1933). The range of the parameter, αr^2 , namely from 1×10^{-9} to 5×10^{-7} m 2 was chosen by bearing in mind the experimental result that the mean radii of air channels varies in a range from 3×10^{-4} to 6×10^{-4} m.

The comparison of the air permeabilities measured for snow at Mizuho Station and Site 2, M and S in Fig. 10, with those calculated for the theoretical model suggests that the decrease in air permeability with decreasing porosity can be reasonably explained by the decrease in the parameter αr^2 ; the decrease in k until p reaches 0.4 is caused mainly by the decrease in r as clearly shown in Fig. 9. This actually means that many interconnecting air voids of complex shape transform to those of simpler and smaller shape due to the mechanical packing process. The decrease in k in a range from $p=0.4$ to $p=0.2$ is considered to be a result of the decrease of

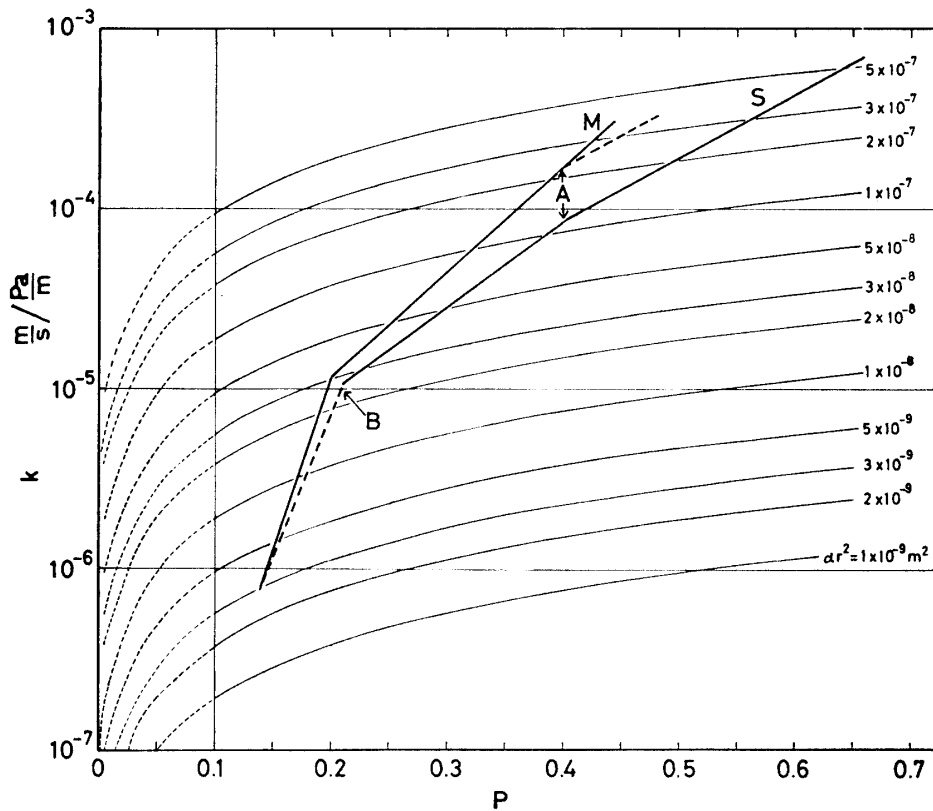


Fig. 10. Theoretical air permeability (k) of ideal snow as a function of porosity (p) and αr^2 , together with the observed results. M : results for the Mizuho snow; S : results for the Site 2 snow.

both r and α . This is because the densification in this porosity range proceeds mainly through the deformation of ice particles to fill up air voids.

The final rapid decrease in k below $p=0.2$ seems to be totally attributable to that in α , that is the splitting or blocking of air channels. This consideration is consistent with various results obtained for the Mizuho cores: MAENO (1974a, 1974b, 1978) has concluded from his electrical measurements that the bonding mode of ice particles reaches an optimum state at a critical density of $730 \text{ kg} \cdot \text{m}^{-3}$ ($p=0.20$), and NARITA *et al.* (1978) have revealed that at the critical density almost all the air voids are concentrated at intersections of grain boundaries; the further densification results in the splitting of air channels, which leads to a rapid decrease in k .

If we assume that the internal texture of the Mizuho snow is such that air channels are randomly distributed, the observed air permeability and porosity give $\alpha r^2=2.27 \times 10^{-7} \text{ m}^2$ at $p=0.4$, $\alpha r^2=3.15 \times 10^{-8} \text{ m}^2$ at $p=0.2$ and $\alpha r^2=4.56 \times 10^{-9} \text{ m}^2$ at $p=0.15$, so that the result in Fig. 9 leads to $\alpha=0.99$, $\alpha=0.27$ and $\alpha=0.04$, respectively. This crude calculation confirms the above explanation of decrease in air permeability with decreasing porosity, and suggests that the optimum state of bond

configuration, as first proposed by MAENO (1974a, 1974b, 1978), corresponds to that in which air channels are contained mainly at intersections of grain boundaries and about 30 per cent of them are unblocked.

Nevertheless, it is not certain what is the most stable configuration of air channels in polar snow which has been maintained for a long time under high hydrostatic pressure and high homologous temperature. There is a possibility that oriented structures are more stable than random ones; among those tetrakaidecahedron-structures are considered to be the most important with respect to the requirement of space-filling (UNDERWOOD, 1970). According to FRANK's (1968) calculation for a volumetric flux through channels in polygranular material composed of grains of truncated octahedron the permeability, k_t is expressed as

$$k_t = \frac{4}{3}k \quad (13)$$

where k is the permeability of a porous material with random configuration of channels, as given by eq. (12).

Finally it should be mentioned that the difference of air permeability observed in snows at Mizuho Station and Site 2 (Figs. 5 and 10) can also be explained in terms of αr^2 . Larger value of αr^2 for the Mizuho snow may be attributed to the climatic characteristics of the Mizuho region, *i.e.* almost stationary strong katabatic wind and small rate of annual accumulation, so that the dominant growth of depth hoar results in the increase in grain size, and in turn an increase in radii of air channels.

Acknowledgments

The authors are indebted to Prof. D. KUROIWA of Hokkaido University for providing them the numerical data of air permeability and elastic modulus of snow measured by the late Dr. U. NAKAYA at Site 2 in Greenland in 1960. They are also indebted to Prof. G. WAKAHAMA of Hokkaido University for his kind encouragement, to Dr. Y. SUZUKI of Hokkaido University and Prof. K. KUSUNOKI of the National Institute of Polar Research for comments on the present paper, and to Mrs. Y. UEMATSU and Mr. Y. KANEDA for their assistance in preparing the manuscript.

The expense of this study was partly defrayed from a Special Fund for Scientific Research of the Ministry of Education, Science and Culture, Japan.

References

- ANDERSON, D. L. and BENSON, C. S. (1963): The densification and diagenesis of snow. *Ice and Snow, Properties, Processes and Applications*, ed. by W. D. KINGERY. Cambridge, The M.I.T. Press, 391–409.
- BADER, H., WATERHOUSE, R. W., LANDUER, J. K., HANSEN, B. L., BENDER, J. A., and BUTKOVICH, T. R. (1955): Excavations and installations at SIPRE test site, Site 2, Greenland. SIPRE

- Tech. Rep., **20**, 32 p.
- BENDER, J. A. (1957): Air permeability of snow. SIPRE Res. Rep., **37**, 19 p.
- BENSON, C. S. (1962): Stratigraphic studies in the snow and firn of the Greenland ice sheet. SIPRE Res. Rep., **70**, 139 p.
- FRANK, F. C. (1968): Two-component flow model for convection in the Earth's upper mantle. Nature, **220**, 350-352.
- KUROIWA, D. (1964): Internal friction of ice. Contrib. Inst. Low Temp. Sci., Hokkaido Univ., Ser. A, **18**, 62 p.
- KUROIWA, D. and KAWAMURA, T. (1974): Jinkô-teki ni atsumitsu shita seppyô to nankyoku seppyô no danseï-ritsu to naibu masatsu (Elastic modulus and internal friction of artificially compressed and Antarctic snow). Kyokuchi Hyôshô-gôri no Butsuri-teki Kagaku-teki Kenkyû (Physical and Chemical Studies on Ices from Glaciers and Ice Sheets), ed. by D. KUROIWA. Sapporo, Inst. Low Temp. Sci., Hokkaido Univ., 15-22.
- MAENO, N. (1974a): Investigations of electrical properties of deep ice cores obtained by drilling in Antarctica. Kyokuchi Hyôshô-gôri no Butsuri-teki Kagaku-teki Kenkyû (Physical and Chemical Studies on Ices from Glaciers and Ice Sheets), ed. by D. KUROIWA. Sapporo, Inst. Low Temp. Sci., Hokkaido Univ., 45-56.
- MAENO, N. (1974b): Kyokuchi no kôri no denki-teki seishitsu I (Electrical properties of polar ice. I). Teion Kagaku, Butsuri-Hen (Low Temp. Sci., Ser. A, Phys.), **32**, 25-38.
- MAENO, N. (1978): The electrical behaviors of Antarctic ice drilled at Mizuho Station, East Antarctica. Mem. Natl Inst. Polar Res., Spec. Issue, **10**, 77-94.
- NAKAYA, U. (1959): Visco-elastic properties of snow and ice in the Greenland ice cap. SIPRE Res. Rep., **46**, 29 p.
- NAKAYA, U. and KUROIWA, D. (1967): Physical properties and internal structure of Greenland snow. Physics of Snow and Ice, ed. by H. ÔURA. Sapporo, Inst. Low Temp. Sci., Hokkaido Univ., 953-971.
- NARITA, H. and MAENO, N. (1978): Compiled density data from cores drilled at Mizuho Station. Mem. Natl Inst. Polar Res., Spec. Issue, **10**, 136-158.
- NARITA, H., MAENO, N. and NAKAWO, M. (1978): Structural characteristics of firn and ice cores drilled at Mizuho Station, East Antarctica. Mem. Natl Inst. Polar Res., Spec. Issue, **10**, 48-61.
- RAYLEIGH, J. W. S. (1929): The Theory of Sound. Vol. 1, London, McMillan, 480 p.
- SMITHSONIAN INSTITUTION (1933): Smithsonian Physical Tables. Eighth revised edition. Washington, 682 p.
- UNDERWOOD, E. E. (1970): Quantitative Stereology. Reading, Addison-Wesley, 274 p.
- YOSIDA, Z., ÔURA, H., KUROIWA, D., HUZIOKA, T., KOJIMA, K., AOKI, S. and KINOSHITA, S. (1956): Physical studies on deposited snow. II. Mechanical properties (1). Contrib. Inst. Low Temp. Sci., Hokkaido Univ., **9**, 74 p.

(Received June 7, 1978; Revised manuscript received September 25, 1978)